Dalton Transactions

COMMUNICATION

Cite this: *Dalton Trans.*, 2014, **43**, 7712

Received 12th January 2014,
Accepted 26th March 2014

DOI: 10.1039/c4dt00101j

www.rsc.org/dalton

Synthesis of dimesitylborane-substituted phenylcarbazoles as bipolar host materials and the variation of the green PHOLED performance with the substituent position of the boron atom†

Hong-Gu Jang, Bo Seong Kim, Jun Yeob Lee and Seok-Ho Hwang*

Two structural isomers of the bipolar host material containing the dimesitylborane moiety were synthesized and their device performance was investigated. The quantum efficiency of the devices depends on the substituent position of the dimesitylborane moiety. The maximum external quantum efficiency of the device reached as high as 23.8% with a green color coordinate of (0.30, 0.63).

For more than ten years, much progress has been made in the field of phosphorescent organic light-emitting diodes (PHOLEDs) because they effectively harvest electro-generated singlet and triplet excitons to accomplish an internal quantum efficiency close to 100%, which is much superior to the 25% upper limit imposed by the formation of singlet excitons in fluorescence.[1] To realize highly efficient PHOLEDs, a suitable host material is usually employed to suppress the intrinsic detrimental effects, such as aggregation quenching and/or triplet–triplet annihilation, of transition metal-centered phosphors.[2] However, designing host materials having higher triplet energy levels than that of the phosphorescent dopant still remains a challenge for materials researchers. Recently, PHOLED-related research has significantly drifted to the development of host materials possessing bipolar properties. With bipolar host materials consisting of both hole- and electron-injecting/transporting functional groups, the wise selection and proper linking of hole- and electron-transporting moieties can promote balancing of the charge fluxes in the devices and alignment of energy levels with the neighboring functional layers, and meanwhile still provide large enough triplet energies compatible with emitters.

One of the most important core structures of bipolar host molecules is the carbazole moiety due to its good hole-transport properties and large triplet energy. To achieve bipolarity in the molecular designs based on carbazole, various moieties capable of electron-accepting, such as pyridine, triazole, triazine, phenanthroline, oxadiazole, benzimidazole, phosphine oxide, and phosphine sulfide, were incorporated to give novel bipolar hosts.[3]

As another electron acceptor, boron-containing derivatives have attracted a great deal of attention due to their intriguing electronic and photophysical properties as a result of the overlap between the vacant p-orbitals of the boron atom.[4] Although these derivatives had been demonstrated to be highly efficient fluorophores,[5] electron-transporting materials,[6] emissive materials,[7] and even bipolar materials in some cases,[5,7*b*,*d*] thus far bipolar phosphorescent host materials based on the combination of phenylcarbazole and dimesitylborane have not been much exploited for green PHOLED devices. In this communication, we reported the synthesis and characterization of novel bipolar and high triplet-energy phosphorescent host materials, 3-(dimesitylboryl)-9-phenyl-9*H*-carbazole (**1**) and 9-(4-(dimesitylboryl)phenyl)-9*H*-carbazole (**3**), that coupled between dimesitylborane and phenylcarbazole to correlate the position of the boron atom of dimesitylborane with the device performance (Scheme 1).

The bipolar host material **1** (33%) was synthesized by the reaction of 3-bromo-*N*-phenylcarbazole first with *n*-butyllithium to give the lithiate intermediate which was subsequently quenched with fluorodimesityl borane. Synthesis of **3** began with the commercially available 9*H*-carbazole, which was *N*-arylated with 1,4-dibromobenzene using the Ullmann coupling reaction to give **2** (36%) that was subsequently treated with *n*-butyllithium and fluorodimesityl borane to form the desired host material **3** (28%). The synthesis of the host materials was confirmed from ^{1}H and ^{13}C NMR, and mass data. The detailed synthetic procedure and analytical methods are described in the ESI.†

The thermal behavior was studied by TGA and DSC under a nitrogen atmosphere. Their glass transition temperatures clearly appeared to be 105 °C (**1**) and 89 °C (**3**), respectively. Also, the decomposition temperatures for the initial 5 wt% loss of mass were 290 °C (**1**) and 296 °C (**3**). These results

---

Department of Polymer Science and Engineering, Dankook University, Yongin, Gyeonggi 448-701, Republic of Korea. E-mail: bach@dankook.ac.kr; Fax: +82 31 8005 3585; Tel: +82 31 8005 3588

† Electronic supplementary information (ESI) available. See DOI: 10.1039/c4dt00101j

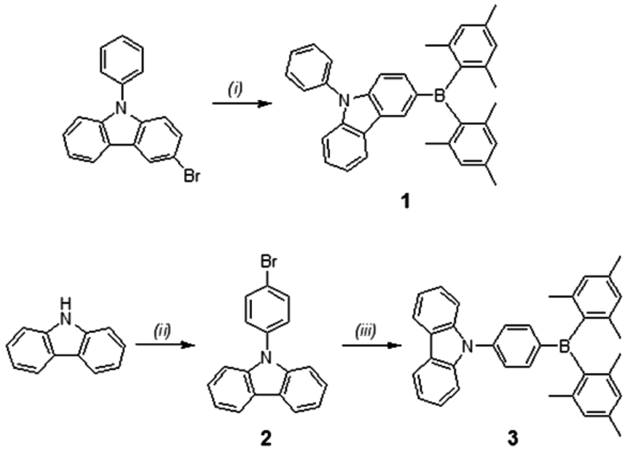

Scheme 1 *Reagents and conditions*: (i) *n*-BuLi, $(Mes)_2BF$, THF, −78 °C to 20 °C; (ii) K_2CO_3, CuI, 18-crown-6, DMF, 130 °C; (iii) *n*-BuLi, $(Mes)_2BF$, THF, −78 °C to 20 °C.

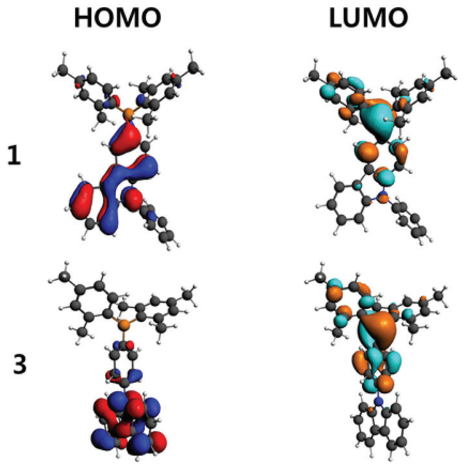

Fig. 1 HOMO and LUMO distribution of **1** and **3**.

mean that they should be suitable to use as a PHOLED component.

Spatial distributions of the HOMO and LUMO orbitals of **1** and **3** were calculated with the Gaussian program at the B3LYP/6-31G(d) level, using the density functional theory (DFT) for the geometry optimizations. As shown in Fig. 1, the HOMO of **1** and **3** is mainly localized at the phenylcarbazole because of the strong electron donating character of nitrogen of carbazole. In contrast, those LUMO showed a different behavior. The LUMO of **3** was localized to the central phenyl and dimesitylborane unit; however, in the case of **1**, a quite extension of the LUMO to the carbazole unit was observed.

Fig. S5† depicts the room temperature absorption and PL spectra of **1** and **3** in various solutions. The absorption spectra in 1,3-dioxane, CH_2Cl_2, acetone and DMSO are almost identical, *i.e.*, independent of the solvent polarity, implying that the Franck–Condon excited-state is subject to a rather small dipolar change with respect to the ground state. On the other hand, the signals in the photoluminescence spectra shifted significantly to longer wavelengths upon increasing the solvent polarity. We attribute this phenomenon to a mechanism involving rapid photoinduced electron transfer between the carbazole donor and the dimesitylborane acceptor units, resulting in a large change in the dipole moment in the excited state; a subsequent solvent relaxation process leads to the solvent polarity-dependent emission.[8] When we plotted the emission peak frequencies of **1** and **3** in various organic solvents as a function of solvent polarities, we obtained an almost linear relationship together with a slope as steep as −4936 (**1**) and −7990 (**3**) cm^{-1}, consistent with our assignment of charge-transfer emission (see Fig. S6 in ESI†).[8] The absorption spectra of **1** and **3** show strong absorption peaks corresponding to π–π^* absorption of the carbazole linked dimesitylborane backbone appearing below 300 nm. Also, two compounds exhibit a strong absorption band around 340 nm assigned to an intramolecular charge transfer (ICT) band from the HOMO delocalized over the carbazole moiety to the LUMO mainly localized on the boron center. In contrast to this similarity in the absorption spectra, significant differences are observed in the fluorescence properties. The solution PL emissions of **1** and **3** were observed at 400 nm and 430 nm, respectively. The wavelength of the emission maximum (λ_{em}) of **3** is more than 30 nm longer than that of **1**. The Stokes shift of **3** exceeds 86 nm (5810 cm^{-1}), whereas that of **1** is only 56 nm (3980 cm^{-1}). This large Stokes shift is one notable characteristic of the present 4-boryl-phenylcarbazole skeleton; presumably, it may be attributed to the change from the twisted structure to the planar structure in the excited state.[7f] The triplet energies of **1** and **3** were 2.88 and 2.72 eV, which could be calculated from the first phosphorescent emission peak of the low temperature (77 K) PL spectrum at 430 and 455 nm, respectively. Their triplet energy was high enough to use the host material as a green phosphorescent dopant. The triplet energy of the tris[2-phenylpyridinato-C^2,*N*]iridium ($Ir(ppy)_3$) dopant is 2.41 eV and effective energy transfer from the synthesized hosts to the $Ir(ppy)_3$ dopant is expected (Fig. 2).

On the basis of the roughly evaluated electrochemical oxidation onset potential, the HOMO levels of **1** and **3** were estimated as −6.21 and −6.17 eV, respectively. Their LUMO levels are −2.86 and −2.95 eV, calculated from the HOMO level and energy bandgap determined from the UV/vis absorption threshold. The LUMO level of **3** was much lower than that of **1** because there may be a different electron accepting ability of the boron center depending on the substituent position onto phenylcarbazole.

Hole- and electron-only devices composed of **1** and **3** were fabricated to compare the hole and electron density in the host materials. Fig. 3 shows the current density–voltage curves of hole- and electron-only devices bearing **1** and **3**. The hole and electron current density of **3** was much higher than those of **1**, which indicates that **3** shows better performance than **1**, in terms of charge transportation. The HOMO and LUMO levels of **1** and **3** were determined to be suitable for hole and electron injection, which accounted for the high hole and elec-

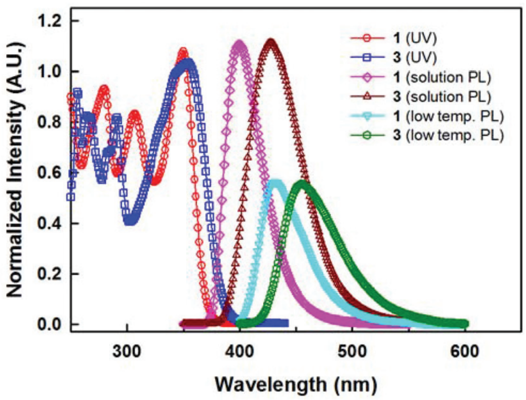

Fig. 2 UV/vis, solution PL and low temp. PL spectra of **1** and **3**.

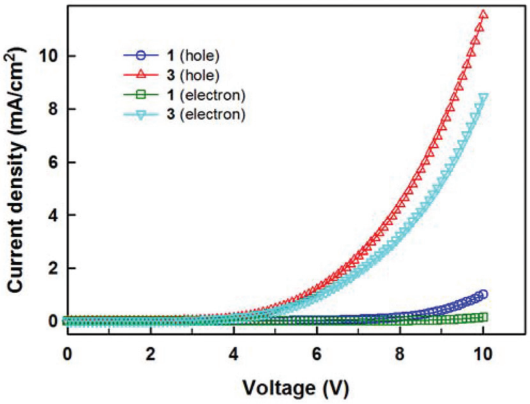

Fig. 3 Current density–voltage of hole- and electron-only devices made of **1** and **3**.

tron current densities with better charge transport properties. Therefore, hole and electron transport properties of **3** were enhanced, resulting in high hole and electron current densities in the hole- and electron-only devices. The better hole transport properties of **3** than that of **1** are due to the localization of the HOMO on carbazole which shows good hole transport properties. The dimesitylborane moiety degraded the hole transport character of carbazole in **1**, which resulted in low hole current density in **1**. Similarly, poor electron transport character of **1** is due to extensive dispersion of the LUMO on the carbazole unit which has poor electron transport properties. In contrast, the LUMO of **3** was localized on the electron deficient phenyl unit modified with dimesitylborane, which improved the electron transport properties of **3**.

The triplet energy of **1** and **3** was suitable for evaluation as the host material of green PHOLEDs. The green PHOLEDs were fabricated using the host materials with 10% of $Ir(ppy)_3$ doping concentration in all devices. Fig. 4(A) shows current density–voltage–luminance curves of the green PHOLEDs. The current density of the green PHOLED with **3** as the host was much higher than that of the green PHOLED with **1** as the host, which is in agreement with the current density–voltage curve of the single carrier devices in Fig. 3. As the hole and electron current densities of the **3** device were higher than those of the **1** device, high current density and luminance were observed for the **3** device. The maximum luminance of the **1** device could not reach 1000 cd m^{-2} compared with over 10 000 cd m^{-2} of the **3** device. Poor charge transport properties of **1** limited the maximum current density and luminance of the **1** device.

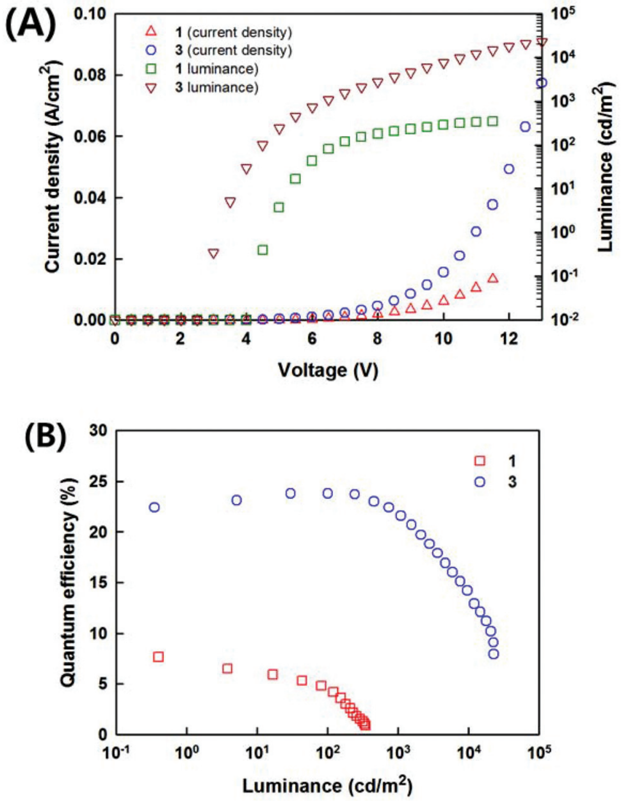

Fig. 4 Current density–voltage–luminance (A) and quantum efficiency–luminance (B) curves of **1** and **3** green PHOLEDs.

External quantum efficiency–luminance curves of the green PHOLEDs are shown in Fig. 4(B). The **3** device exhibited much higher quantum efficiency than the **1** device at the same luminance. The maximum quantum efficiency and the quantum efficiency at 1000 cd m^{-2} of the **3** device were 23.8% and 21.7% compared with the maximum quantum efficiency of 6.5% of the **1** device. There was more than three times improvement of the quantum efficiency of the **3** device. The high quantum efficiency of the **3** device is related to balanced charge density, exciton confinement and efficient energy transfer. As shown in the single carrier device data in Fig. 3, the hole current density of **3** was similar to the electron current density of **3**, which indicates bipolar charge transport properties. The bipolar charge transport properties of **3** balanced holes and electrons in the emitting layer, which contributed to the high quantum efficiency of the **3** device. However, the hole current density was much higher than the electron current density in the **1** device, which leads to poor charge balance and low quantum efficiency. Exciton confinement by the high

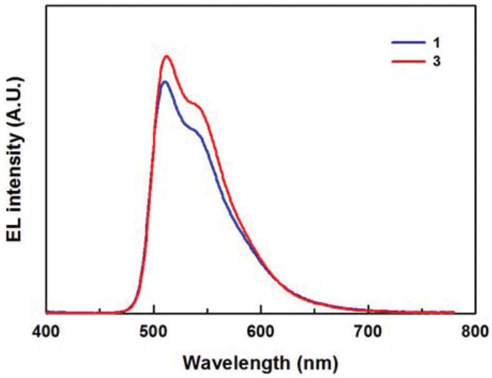

Fig. 5 EL spectra of **1** and **3** green PHOLEDs.

triplet energy host, hole transport material and electron transport material also played an important role in enhancing the quantum efficiency of the **3** device. As the triplet energy of the host and charge transport materials was higher than that of Ir(ppy)$_3$, triplet excitons of Ir(ppy)$_3$ could be effectively confined in the emitting layer with little quenching. Finally, efficient energy transfer as can be observed in the electroluminescence (EL) spectrum of the **3** device in Fig. 5 was another key factor for the high quantum efficiency of the **3** device. Only green emission of Ir(ppy)$_3$ without any emission from the **3** host material was observed in the EL spectra, implying good energy transfer from the **3** host to Ir(ppy)$_3$. The low quantum efficiency of the **1** device is due to poor charge balance in the emitting layer because excitons can be effectively confined in the **1** device and no emission from the **1** host was observed in the EL spectrum of the **1** device.

EL spectra of the **1** and **3** devices are shown in Fig. 5. Strong green emission by Ir(ppy)$_3$ appeared at 509 nm with a shoulder at 539 nm. No other emission peaks from host or charge transport materials were observed, confirming effective charge confinement in the emitting layer. Color coordinates of the **1** and **3** devices were (0.31, 0.62) and (0.30, 0.63), respectively.

Conclusions

In summary, two structural isomers, 3-(dimesitylboryl)-9-phenyl-9*H*-carbazole and 9-(4-(dimesitylboryl)phenyl)-9*H*-carbazole, with the dimesitylboryl group at different positions of the phenylcarbazole moiety, were synthesized. Thereof, the photophysical properties and device performances were correlated with the molecular structure. The maximum quantum efficiency and the quantum efficiency at 1000 cd m^{-2} of the device with **3** were 23.8% and 21.7% compared with the maximum quantum efficiency of 6.5% of the device with **1**. Therefore, the dimesitylboryl group should be selectively introduced into the molecular structure of host materials to manage the charge transport properties of host materials.

Acknowledgements

The present research was supported by the research fund of Dankook University in 2012 (grant no. 108863).

Notes and references

1 (*a*) J. Kido, M. Kimura and K. Nagai, *Science*, 1999, **267**, 1332; (*b*) S. R. Forrest, *Org. Electron.*, 2003, **4**, 45; (*c*) W. D'Andrade and S. R. Forrest, *Adv. Mater.*, 2004, **16**, 1585; (*d*) Y. Chi and P.-T. Chou, *Chem. Soc. Rev.*, 2010, **39**, 638.

2 (*a*) M. A. Baldo, C. Adachi and S. R. Forrest, *Phys. Rev. B: Condens. Matter*, 2000, **62**, 10967; (*b*) S.-J. Su, H. Sasabe, T. I. Takeda and J. Kido, *Chem. Mater.*, 2008, **20**, 1691.

3 (*a*) S.-J. Su, C. Cai and J. Kido, *Chem. Mater.*, 2011, **23**, 274; (*b*) M. K. Kim, J. Kwon, T.-H. Kwon and J.-I. Hong, *New J. Chem.*, 2010, **34**, 1317; (*c*) Z. Q. Gao, M. Luo, X. H. Sun, H. L. Tam, M. S. Wong, B. X. Mi, P. F. Xia, K. W. Cheah and C. H. Chen, *Adv. Mater.*, 2009, **21**, 688; (*d*) Y. Tao, Q. Wang, L. Ao, C. Zhong, J. Qin, C. Yang and D. Ma, *J. Mater. Chem.*, 2010, **20**, 1759; (*e*) Z. Ge, T. Hayakawa, S. Ando, M. Ueda, T. Akiike, H. Miyamoto, T. Kajita and M. Kakimoto, *Adv. Funct. Mater.*, 2008, **18**, 584; (*f*) S. O. Jeon, S. E. Jang, H. S. Son and J. Y. Lee, *Adv. Mater.*, 2011, **23**, 1436.

4 (*a*) J.-L. Bredas, J. E. Norton, J. Cornil and V. Coropceanu, *Acc. Chem. Res.*, 2009, **42**, 1691; (*b*) C. D. Entwistle and T. B. Marder, *Angew. Chem., Int. Ed.*, 2002, **41**, 2927; (*c*) S. Yamaguchi, T. Shirasake, S. Akiyama and K. Tamao, *J. Am. Chem. Soc.*, 2002, **124**, 8816; (*d*) S. K. Murphy, C. Baik, J.-S. Lu and S. Wang, *Org. Lett.*, 2010, **12**, 5266; (*e*) H. Pan, G.-L. Fu, Y.-H. Zhao and C.-H. Zhao, *Org. Lett.*, 2010, **12**, 5192; (*f*) S.-C. Lo and P. L. Burn, *Chem. Rev.*, 2007, **107**, 1097.

5 S. L. Lin, L. H. Chan, R. H. Lee, M. Y. Yen, W. J. Kuo, C. T. Chen and R. J. Jeng, *Adv. Mater.*, 2008, **20**, 3947.

6 (*a*) A. Wakamiya, T. Taniguchi and S. Yamaguchi, *Angew. Chem., Int. Ed.*, 2006, **45**, 3170; (*b*) D. Tanaka, T. Takeda, T. Chiba, S. Watanabe and J. Kido, *Chem. Lett.*, 2007, **36**, 262.

7 (*a*) T. Noda, H. Ogawa and Y. Shirota, *Adv. Mater.*, 1999, **11**, 283; (*b*) Y. Shirota, M. Kinoshita, T. Noda, K. Okumoto and T. Ohara, *J. Am. Chem. Soc.*, 2000, **122**, 11021; (*c*) M. Kinoshita and Y. Shirota, *Chem. Lett.*, 2001, **30**, 614; (*d*) H. Doi, M. Kinoshita, K. Okumoto and Y. Shirota, *Chem. Mater.*, 2003, **15**, 1080; (*e*) M. Mazzeo, V. Vitale, F. D. Sala, M. Anni, G. Barbarella, L. Favaretto, G. Sotgiu, R. Cingolani and G. Gigli, *Adv. Mater.*, 2005, **17**, 34; (*f*) A. Wakamiya, K. Mori and S. Yamaguchi, *Angew. Chem., Int. Ed.*, 2007, **46**, 4273.

8 (*a*) Y. Y. Chien, K. T. Wong, P. T. Chou and Y. M. Cheng, *Chem. Commun.*, 2002, 2874; (*b*) K. T. Wong, S. Y. Ku, Y. M. Cheng, X. Y. Lin, Y. Y. Hung, S. C. Pu, P. T. Chou, G. H. Lee and S. M. Peng, *J. Org. Chem.*, 2006, **71**, 456.